

Sodium-potassium system at high pressure

Mungo Frost,¹ Emma E. McBride,¹ Maximilian Schörner,² Ronald Redmer^{⊗,2} and Siegfried H. Glenzer¹

¹SLAC National Accelerator Laboratory, 2575 Sand Hill Road, Menlo Park, USA

²Institut für Physik, Universität Rostock, 18051 Rostock, Germany



(Received 17 March 2020; accepted 20 May 2020; published 9 June 2020)

Mixtures of sodium and potassium differ substantially from the pure elements, while retaining the high compressibility, which is important to the complex behavior of dense alkali metals. We present powder x-ray diffraction of mixtures of Na and K compressed in diamond anvil cells to 48 GPa at 295 K. This reveals two stoichiometric intermetallics: an Na₂K phase known at ambient pressure and low temperature, and a novel NaK phase formed of interpenetrating sodium and potassium diamond lattices. Density functional theory calculations find the new phase to be dynamically stable and, in contrast to pure alkali metals, reveal decreasing electron localization with applied pressure. Depending on the mixture composition these intermetallics are accompanied by sodium or potassium rich phases suggesting that there are no other intermetallics under the range of *P-T* conditions studied. Alkali-metal mixtures have seen little study at high pressure and represent an unusual class of materials with very high compressibility and multiple constituents. Such materials exhibit significant compression at experimentally accessible pressures and open a way to measure multispecies structures at high compression. These results challenge structural finding algorithms for mixtures in high-pressure conditions.

DOI: [10.1103/PhysRevB.101.224108](https://doi.org/10.1103/PhysRevB.101.224108)

I. INTRODUCTION

Alkali metals exhibit a range of remarkable behaviors under pressure. At ambient conditions they are simple *bcc* metals with nearly free electron behavior. On compression they all exhibit local minima in their melting curves [1–5] and their solids adopt complex, low-symmetry structures around the same pressure [6–10]. Host-guest structures, in which a host lattice contains guest atoms of the same element, have been observed in rubidium, potassium, and sodium [8,9,11], while at higher pressure the opening of a band gap and loss of metallic behavior is reported [12,13].

The unusual high-pressure behaviors observed in the alkali metals are in part related to their low bulk moduli, which allows for significant compression to be reached at experimentally accessible pressures. Similar turnovers in the melt curve have been predicted in magnesium and aluminium at much higher pressures, and may be more universal than was previously thought [14]. Likewise elemental electride structures, in which localized electron density plays the role of a pseudo-anion, have been reported in the alkali metals [12,15], and predicted in other elements at extreme pressures [16,17]. Interactions between core and valence electrons appear to have a key role in causing the complex behaviors observed at high compression [17,18].

Here we investigate binary mixtures of sodium (Na) and potassium (K) at high pressures and find a novel intermetallic. These mixtures share the high compressibility of the pure elements but have two species present, which changes the phases and properties of the system. The components also cover two regimes of core valence overlap: in potassium, and heavier alkali elements, *s* → *d* charge transfer is important in their high-pressure behavior [19]. In sodium the highest occupied orbital is the 3*s*, which lies at significantly lower

energy than the 3*d*, though *p* → *d* charge transfer is predicted to become important at high pressure [12].

Sodium-potassium alloys have a number of practical applications. Mixtures with 30–83 atomic % potassium are liquid at room temperature, with the eutectic at 66.6 atomic % potassium melting at −12 °C [20]. It is used as a coolant in some nuclear reactors where it has the advantage over pure sodium of not freezing in the coolant circuit upon shutdown [21]. It is also used as a desiccant in chemistry [22], and as a hydraulic fluid [23]. On freezing at ambient pressure there is a single intermetallic phase of stoichiometry Na₂K, which crystallizes into a hexagonal Laves phase of space group *P6₃/mmc*, which is isostructural with MgZn₂ [24].

A few other binary intermetallics of alkali elements and cesium are known [25,26], including a structure LiCs, which is stabilized by the application of pressure [26]. Na₂Cs and K₂Cs have both also been observed to adopt a similar *P6₃/mmc* structure to Na₂K showing trends in the intermetallics, which form in the alkali metals [25]. High-pressure investigation of sodium-potassium alloys has been limited to date. An experimental study considered the evolution of the eutectic and peritectic temperature to 6 GPa, though does not present structural data [27]. More recently a theoretical paper [28] considered the high-pressure structures at fixed Na₂K stoichiometry. It finds the known *P6₃/mmc* phase stable to 10 GPa where a transition to a *P3̄m1* phase is predicted prior to the demixing of the sodium and potassium at 37 GPa.

The experimental results reported here agree only on the presence of a low-pressure *P6₃/mmc* phase, which is observed between 0.9 and 5.9 GPa. Above this pressure the sodium-potassium system no longer forms compounds of stoichiometry Na₂K, rather we observe a stoichiometric NaK intermetallic to at least 48 GPa, accompanied by mixed *bcc* phases, which have not been considered by the previous

theory paper [28]. Our new density functional theory (DFT) calculations reproduce the experimentally determined pressure-volume relation very well and find the proposed structure to be dynamically stable over the full range of pressures in which it is observed.

II. METHODS

Liquid sodium-potassium alloys of molar compositions Na:2K, Na:K, and 2Na:K were prepared from the pure metals in a high-purity argon glove box. This range of compositions covers sodium-rich, potassium-rich and equal to investigate the effect of composition as well as measuring the known stoichiometric phase, Na₂K, and the eutectic point close to 66 atomic % K, which is most relevant to practical applications. To prepare the mixtures appropriate quantities of metallic sodium (99.95%, Alfa Aesar) and potassium (99.95%, Alfa Aesar) were weighed into vials where the solid sodium and potassium metals fully liquified over a few minutes as they mixed. They were then thoroughly stirred with a glass rod and stored in the glove box for at least one week to ensure complete mixing.

Diamond anvil cells were prepared with 400 or 200 μm culets and rhenium gaskets. Pressure was determined with uncertainty of 0.1 GPa via the equation of state of a small flake of tungsten included in each sample [29]. The liquid sodium-potassium mixture was then loaded under a high-purity argon atmosphere. Ruby was avoided due to the potential for reactions, and pressure transmitting media were omitted due to both the possibility of reaction and technical difficulty in loading it with a highly reactive liquid metal sample. Inspection of the diamond anvil culets under a polarizing microscope after the experiment revealed no indication of reaction or degradation of the diamonds by the samples. No evidence of reaction with the rhenium gaskets or tungsten pressure marker was observed.

Angular dispersive powder x-ray diffraction was carried out at APS beamline 16-BM-D (HP-CAT) using 0.4133 Å radiation. The load was increased in steps using a gas membrane to around 23 GPa (400 μm culets) and 48 GPa (200 μm culets) with diffraction data collected on a large area detector. To optimize the quality of the powder data the cell position was rastered in a plane perpendicular to the beam by 25 or 50 μm , with the area chosen to avoid the rhenium gasket. All data were collected at ambient temperature, ≈ 295 K. The resultant patterns were radially integrated using the DIOPTAS software package [30]. LeBail fits were then performed using JANA2006 [31]. Structure visualization was performed using VESTA [32].

Density functional theory (DFT) calculations for the $Fd\bar{3}m$ NaK phase were performed using the Perdew-Burke-Ernzerhof functional [33] as implemented in VASP [34–37]. We employed the projector augmented wave method with nine electrons for both sodium and potassium, while the remaining electrons were frozen in the core. All calculations were carried out with a plane wave energy cutoff of 1000 eV and a self-consistent field energy convergence of 10^{-8} eV. The k -point sampling was performed according to the technique of Monkhorst and Pack [38]. The phonon density of states was computed using the harmonic approximation implemented in

phonopy [39] where the dynamical matrix was evaluated at a $31 \times 31 \times 31$ k -point set. The pressure-volume relation was computed for a cell of 16 atoms (Na on the $8a$ Wyckoff positions and K on the $8b$ Wyckoff positions) and a $7 \times 7 \times 7$ k -point set, whereas the phonon density of states and electron localization function (ELF) [40] were calculated for a $2 \times 2 \times 2$ supercell (128 atoms) with a $5 \times 5 \times 5$ k -point set.

III. EXPERIMENTAL RESULTS AND DISCUSSION

Sodium and potassium mixtures were compressed at room temperature to a maximum pressure of 48 GPa in diamond anvil cells (DACs). Angular dispersive powder x-ray diffraction data was collected at the Advanced Photon Source (APS) using a monochromatic beam ($\lambda = 0.4133$ Å) to study their structural evolution. Mixtures of molar compositions Na:2K, Na:K, and 2Na:K were studied. Here, the nomenclature Na:K refers to a sodium-potassium mixture of equal atomic ratio, while NaK refers to a stoichiometric intermetallic phase. The range of mixtures studied covers sodium-rich, potassium-rich, and equal to investigate the effect of composition.

All the mixtures studied are liquids at ambient pressure and freeze around 1 GPa. Prior to freezing, clear liquid diffraction was observed (Supplemental Material, Fig. S1) while at pressures above this a mixture of the known Na₂K $P6_3/mmc$ phase and excess bcc alkali metal was observed in all samples. The x-ray diffraction pattern and LeBail fit for the 2Na:K mixture is shown in Fig. 1 (top). For the Na:K and Na:2K mixtures the pressure-volume data of the bcc peaks lie close to that of potassium [43] suggesting a potassium-rich phase, while for the 2Na:K mixture exhibited peaks indicating a sodium-rich bcc phase [44]. In the latter case this could indicate either sodium deficiency in the Na₂K phase or that the 2Na:K mixture was slightly rich in sodium. Pressure-volume curves are shown in Fig. 2 and the bcc phases discussed further below. The $P6_3/mmc$ phase is known to form below 280 K at zero pressure [20] therefore it is not unexpected that it forms on freezing of the liquid at room temperature on compression, which is in agreement with previous theoretical predictions [28].

On compression above 5.9(1) GPa both the 2Na:K and Na:K mixtures undergo a phase transition. All observed peaks are fitted very well by an $Fd\bar{3}m$ phase, $a = 7.222(1)$ Å at 17 GPa, with an excess bcc sodium-rich phase. The data and fit for the Na:K mixture are shown in Fig. 1 (middle). Consideration of density and symmetry allow a full structural solution to be inferred. The lowest multiplicity Wyckoff positions of the $Fd\bar{3}m$ space group are the $8a$ and $8b$ positions. Occupation of higher multiplicity positions can be excluded as it would lead to an unrealistically high density, see Fig. 3. This in turn implies that the phase has equal stoichiometry NaK and, as neither of the occupied positions has any adjustable parameters, uniquely specifies a structure, which is shown in Fig. 4. This structure is uncommon, but has been observed in a few sodium compounds and is referred to as a NaTl (sodium thallide) or B32-type structure [46]. Analysis of the lattice parameter of the excess bcc phase in the Na:K mixture yields further evidence of a change in stoichiometry of the intermetallic. Around 5.9 GPa there is a discontinuous change, which corresponds to a transition from a potassium-rich bcc

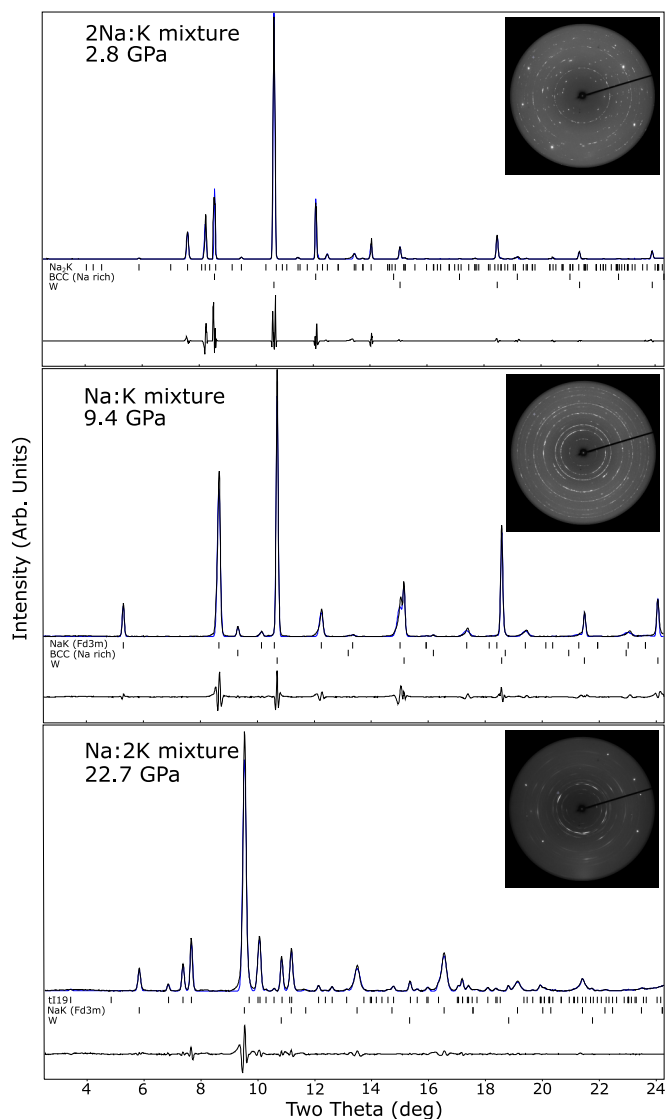


FIG. 1. Top: integrated powder pattern of a 2Na:K molar ratio mixture at 2.8 GPa. Background subtracted data (black) with LeBail fit (blue) and residual (below). Ticks indicate possible peak locations of $P6_3/mmc$ Na_2K , a sodium-rich bcc phase, and tungsten as marked. The unintegrated pattern is inset. The Na_2K phase has lattice parameters $a = 6.768(1)$ Å and $c = 11.051(2)$ Å. Middle: a similar plot for an equimolar Na:K mixture at 9.4 GPa showing the novel $Fd\bar{3}m$ NaK phase, a sodium-rich bcc phase and tungsten. Bottom: a similar plot for a Na:2K mixture at 22.7 GPa showing $tI19$ potassium, $Fd\bar{3}m$ NaK and tungsten. The $tI19$ ticks are for the host lattice only. Asymmetric broadening in the $Fd\bar{3}m$ NaK phase is fitted using Stephen's method [41] in both cases and is attributed to strain. Additional diffraction data is presented in the Supplemental Material [42].

phase to a sodium-rich one, see Fig. 2, implying that the potassium content of the intermetallic increased. The $Fd\bar{3}m$ NaK phase remains to at least 48 GPa, the highest pressure measured.

The sodium-rich bcc phase observed in the 2Na:K and Na:K mixtures has a lattice parameter slightly exceeding that of pure sodium [44], see Fig. 2. This may be attributed to the

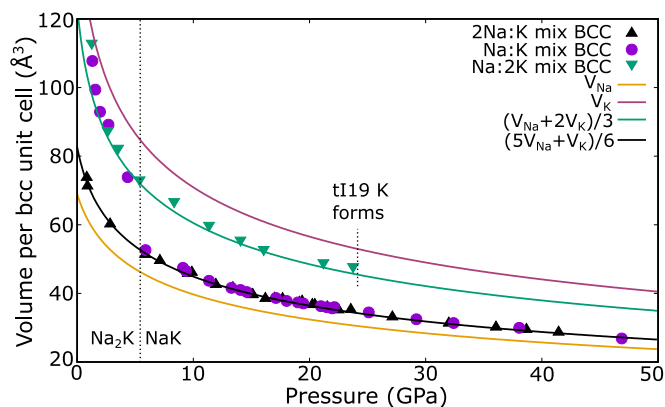


FIG. 2. Pressure-volume curves for the bcc phases. Vertical axis is volume per two atoms corresponding to one unit cell of bcc . The coexisting intermetallic transitions from Na_2K to NaK at 5.9 GPa as indicated, this change in stoichiometry coincides with a discontinuity in the lattice parameter of the excess bcc phase in the Na:K mixture as it goes from K-rich to Na-rich. Pressure-volume curves for bcc sodium [44] and bcc potassium [43] use the Holzapfel $H02$ equation of state [45]. Error bars are smaller than plotting points.

inclusion of potassium into the bcc structure. The observed lattice parameter is well fitted by a linear combination of the equations of state of bcc sodium [44] and bcc potassium [43], in the ratio of $(5V_{\text{Na}} + V_{\text{K}})/6$ for both 2Na:K and Na:K mixtures. The excess sodium-rich phase has very similar lattice parameters for both mixtures meaning that both have a similar concentration of potassium atoms replacing sodium atoms. No additional diffraction peaks are observed, which suggests the potassium is not ordered on the lattice and that there is a preferred solubility of the $Fd\bar{3}m$ NaK intermetallic into the sodium-rich bcc phase with the result that the sodium-rich bcc phase will always have the same potassium concentration when in coexistence with NaK.

The potassium-rich Na:2K mixture exhibited different behavior on compression. The mixture of a potassium-rich bcc

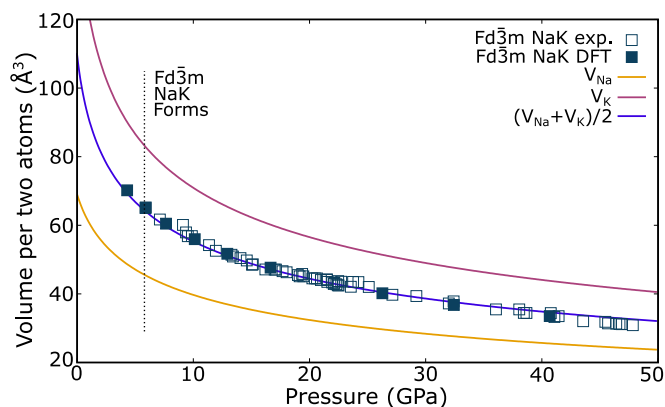


FIG. 3. Experimental and simulated pressure-volume relations for $Fd\bar{3}m$ NaK show close agreement. Vertical axis is volume per two atoms corresponding to one formula unit of $Fd\bar{3}m$ NaK or one bcc unit cell of the pure elements. Pressure-volume curves for bcc sodium [44] and bcc potassium [43] use the Holzapfel $H02$ equation of state [45]. Error bars are smaller than plotting points.

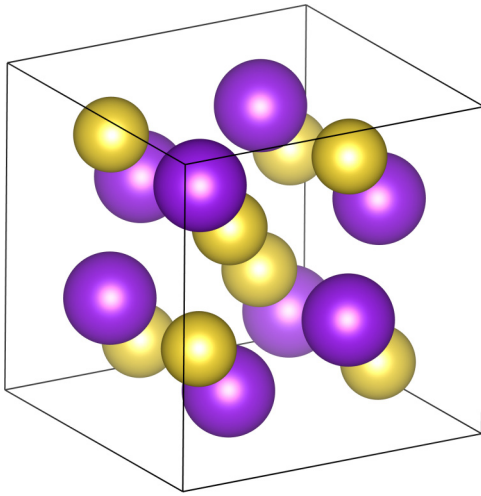


FIG. 4. Unit cell of the high-pressure $Fd\bar{3}m$ NaK phase. Sodium atoms are in yellow, potassium in purple.

phase and the low pressure $P6_3/mmc$ Na_2K phase obtained on freezing persists to only 3 GPa where the peaks due to the $P6_3/mmc$ phase are lost. The resulting bcc phase has a smaller lattice parameter than is observed in pure potassium, and is fitted well by a linear combination of the equations of state of sodium [44] and potassium [43] in ratio $(V_{Na} + 2V_K)/3$ suggesting a potassium-rich mixed bcc phase, see Fig. 2. This ratio matches the ratio of the elements in the mixture. The absence of additional diffraction peaks suggests that there is no loss of symmetry and the sodium and potassium atoms are randomly distributed on the bcc lattice.

This mixed bcc phase persists on compression to 24 GPa at which point it transforms to a mixture of $tI19$ potassium [8] and the $Fd\bar{3}m$ NaK phase observed above 6 GPa in the other mixtures. The diffraction pattern and LeBail fit are shown in Fig. 1 (bottom). Pure potassium transforms from bcc to fcc at 11 GPa and then to $tI19$ at 19 GPa [8]. The addition of sodium completely suppresses the formation of fcc potassium and delays the formation of the $tI19$ phase to 24 GPa. On decompression of the Na:2K mixture $tI19$ potassium is observed to 20.5 GPa, the lowest pressure before the cell opened. This suggests that the bcc mixture may be metastable over at least some of the pressure range it is observed in. The binary phase diagram for the Na-K system is shown in Fig. 5.

$tI19$ potassium is an incommensurate host-guest structure in which a host lattice contains chains of guest atoms [8]. The host lattice has 16 atoms per unit cell and space group $I4/mcm$, which is indexed here. Host-guest and guest-only x-ray diffraction reflections are weak [8], and both sublattice melting of the guest chains [2], and a transition in the guest structure at 30 GPa [47] are known. Their very low intensity, and the large range of 2θ , which is covered by other peaks, see Fig. 1 (bottom), makes unambiguous fitting of the guest peaks impossible so the guest structure and composition cannot be determined.

The volume of both the sodium- and potassium-rich bcc phases is well described by a linear combination of the equations of state of the bcc phases of the pure elements over a range of pressures, Fig. 2. The atoms are situated

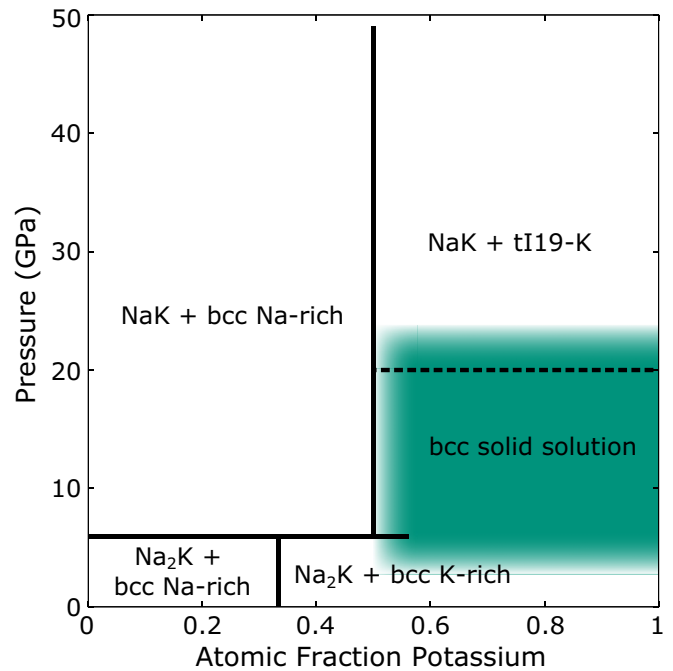


FIG. 5. Binary phase diagram of the Na – K system at 295 K. The green shaded region corresponds to the solid solution, which may be metastable over at least some of the area it covers.

on the same lattice in the mixed bcc phases and the pure elements so they may be expected to occupy a similar volume. From this the composition of each mixture can be estimated: (i) The potassium-rich bcc phase is well approximated by two parts potassium to one part sodium, matching the composition of the mixture, which was loaded in the cell. (ii) The sodium-rich bcc phase appears to favor a 5:1 composition of sodium:potassium in both the 2Na:K and Na:K mixtures when in coexistence with the $Fd\bar{3}m$ NaK intermetallic. The weak sodium-rich bcc peaks in the equal composition Na:K mixture implies either nonstoichiometric sodium deficiency in $Fd\bar{3}m$ NaK, or a slight excess of sodium in the Na:K mixture. In both cases, though, the $Fd\bar{3}m$ NaK dissolves into excess sodium to give the same composition of the bcc sodium-rich phase. Solid solutions are known in the K-Rb and Rb-Cs binary alkali-metal systems under ambient conditions [48].

The experimental results are in contrast to previous DFT predictions [28]. At low pressures experimental results and theoretical predictions are in agreement, both showing that the known $P6_3/mmc$ Na_2K intermetallic is formed. However, the previous DFT study did not account for stoichiometries other than Na_2K and so could not have found the $Fd\bar{3}m$ NaK phase. Their predicted high-pressure $P\bar{3}m1$ Na_2K phase is not observed, and demixing of the sodium and potassium is excluded to at least 48 GPa, considerably above the 37 GPa suggested in their study.

The NaTl structure adopted by NaK has a number of unusual properties. It is shown in Fig. 4 and is comprised of two interpenetrating diamond lattices, one of sodium and one of potassium. Each atom has eight nearest neighbors, four sodium and four potassium. Having equal numbers of like and unlike nearest neighbors is unusual, though it should be

noted that each atom has a second shell of six next-nearest neighbors at 1.15 times the distance of the first shell, all of which are of the other species. Nearest neighbors occur in the $\langle 111 \rangle$ directions with a pattern of alternating pairs: that is the ordering . . . - Na - Na - K - K - Na - Na - . . .

IV. DENSITY FUNCTIONAL THEORY RESULTS AND DISCUSSION

The properties of $Fd\bar{3}m$ NaK have been further investigated using DFT simulations. The calculated pressure-volume relation is shown in Fig. 3 along with experimental data. It can be seen that agreement between experiment and theory is excellent, which lends confidence when theory is extended to properties less easily approached experimentally. The phonon density of states of NaK has been calculated at lattice parameters of 8.25 Å and 6.25 Å, corresponding to calculated pressures of 4.3 GPa and 50.6 GPa, respectively; covering the range of pressures at which the phase was experimentally observed. These are shown in Fig. 6 and exhibit no imaginary modes implying that the structure is dynamically stable.

The electron localization function (ELF) [40] has also been mapped for both densities and is shown in Fig. 7. At lower density biconcave hexagonal pancakes of electron localization lie between nearest-neighbor sodium atoms, but similar localization is not present between sodium-potassium or potassium-potassium nearest neighbors. This may be explained as all nearest-neighbor distances are the same, while sodium atoms are smaller than potassium, meaning the spaces between them offer larger interstitial volume. The application of pressure suppresses this localization and it is not observed at the higher density. This is in contrast to pure alkali metals, which generally show increasing interstitial electron localization at high pressure, attributed to core-valence overlap [17,49,50].

The unusual structure of $Fd\bar{3}m$ NaK may explain the reduced localization on increasing pressure. The nearest-neighbor distances are the same for sodium-sodium, sodium-potassium, and potassium-potassium pairs with the result of there are a range sizes of interstitial spaces. Due to the smaller size of sodium the spaces between sodium pairs will be larger. However, as pressure is increased these spaces become smaller. The loss of interstitial electron localization

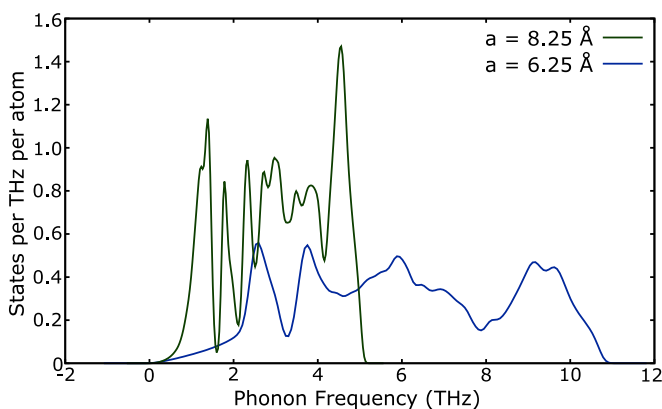


FIG. 6. The phonon density of states for $Fd\bar{3}m$ NaK at low and high pressure show the proposed structure to be dynamically stable.

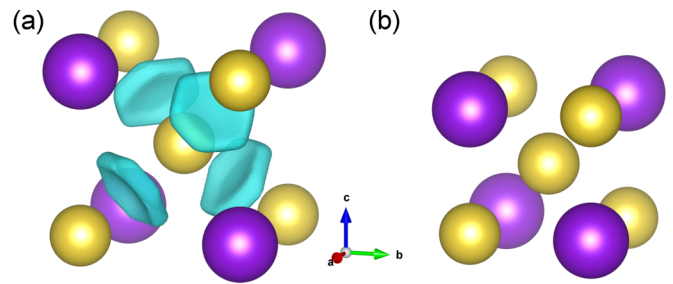


FIG. 7. The 0.6 isosurface of the electron localisation function around a sodium atom in $Fd\bar{3}m$ NaK. The isosurface from adjacent sodium-sodium interstitials and near the potassium atoms is omitted for clarity. (a) with lattice parameter of 8.25 Å, corresponding to a calculated pressure of 4.3 GPa. (b) with lattice parameter of 6.25 Å, corresponding to a calculated pressure of 50.6 GPa. The hexagonal disks of electron localization between nearest neighbor sodium atoms disappear at higher pressure where there is no significantly localised interstitial electron density. Inset arrows show crystallographic axes; sodium atoms are yellow, potassium purple and the isosurface is teal.

in $Fd\bar{3}m$ NaK occurs at lower pressure than significant core-valence overlap effects are observed in the pure elements. It is therefore possible that electron localization may reappear at higher pressures, if sodium-potassium intermetallics remain stable.

V. CONCLUSION

The sodium-potassium system has been investigated at room temperature to 48 GPa with molar ratios of 2:1, 1:1, and 1:2 Na:K. The liquid metals freeze close to 1 GPa to form a Na_2K $P6_3/mmc$ phase, which is known from freezing at ambient pressure and low temperature [20]. At pressures above 5.9(1) GPa a novel stoichiometric NaK intermetallic with space group $Fd\bar{3}m$ forms. This persists to at least 48 GPa in coexistence with sodium- or potassium-rich phases suggesting the absence of other stoichiometric intermetallics under the conditions studied. Substantial solid solubility of each of sodium and potassium into the bcc phase of the other is observed without detectable symmetry lowering, and with the complete suppression of the fcc transition of potassium by the addition of sodium. New DFT calculations find the $Fd\bar{3}m$ phase to be dynamically stable and, in contrast to the pure species, it exhibits decreased interstitial electron localization at higher pressure. Given the highly complex behavior of the pure elements, alkali-metal mixtures under pressure is an intriguing field, which has only very recently been approached. A prior *ab initio* structure search did not find the novel $Fd\bar{3}m$ NaK phase [28]. It therefore forms a test to future theoretical studies on mixed alkali-metal systems under extreme pressure, and more generally compressed mixtures which are of great importance, for example in modeling planetary interiors.

ACKNOWLEDGMENTS

The authors would like to thank Changyong Park and Mandy Bethkenhagen. This work was supported by

U.S. Department of Energy (DOE) Office of Fusion Energy Sciences Funding No. FWP100182. Equipment support from Stanford Synchrotron Radiation Light source (SSRL) is acknowledged under DOE Office of Basic Energy Sciences under Contract No. DE-AC02-76SF00515. Powder XRD was performed at HPCAT (Sector 16), Advanced Photon Source (APS), Argonne National Laboratory. HPCAT operations are

supported by DOE-NNSA's Office of Experimental Sciences. The Advanced Photon Source is a DOE Office of Science User Facility operated for the DOE Office of Science by Argonne National Laboratory under Contract No. DE-AC02-06CH11357. The *ab initio* calculations were performed at the North-German Supercomputing Alliance (HLRN) facilities.

- [1] H. Luedemann and G. Kennedy, *J. Geophys. Res.* **73**, 2795 (1968).
- [2] E. E. McBride, K. A. Munro, G. W. Stinton, R. J. Husband, R. Briggs, H.-P. Liermann, and M. I. McMahon, *Phys. Rev. B* **91**, 144111 (2015).
- [3] E. Gregoryanz, O. Degtyareva, M. Somayazulu, R. J. Hemley, and H.-k. Mao, *Phys. Rev. Lett.* **94**, 185502 (2005).
- [4] A. M. J. Schaffer, W. B. Talmadge, S. R. Temple, and S. Deemyad, *Phys. Rev. Lett.* **109**, 185702 (2012).
- [5] M. Frost, J. B. Kim, E. E. McBride, J. R. Peterson, J. S. Smith, P. Sun, and S. H. Glenzer, *Phys. Rev. Lett.* **123**, 065701 (2019).
- [6] M. I. McMahon, R. J. Nelmes, and S. Rekhi, *Phys. Rev. Lett.* **87**, 255502 (2001).
- [7] R. J. Nelmes, M. I. McMahon, J. S. Loveday, and S. Rekhi, *Phys. Rev. Lett.* **88**, 155503 (2002).
- [8] M. I. McMahon, R. J. Nelmes, U. Schwarz, and K. Syassen, *Phys. Rev. B* **74**, 140102(R) (2006).
- [9] E. Gregoryanz, L. F. Lundegaard, M. I. McMahon, C. Guillaume, R. J. Nelmes, and M. Mezouar, *Science* **320**, 1054 (2008).
- [10] C. L. Guillaume, E. Gregoryanz, O. Degtyareva, M. I. McMahon, M. Hanfland, S. Evans, M. Guthrie, S. V. Sinogeikin, and H. Mao, *Nature Phys.* **7**, 211 (2011).
- [11] U. Schwarz, A. Grzechnik, K. Syassen, I. Loa, and M. Hanfland, *Phys. Rev. Lett.* **83**, 4085 (1999).
- [12] Y. Ma, M. Eremets, A. R. Oganov, Y. Xie, I. Trojan, S. Medvedev, A. O. Lyakhov, M. Valle, and V. Prakapenka, *Nature (London)* **458**, 182 (2009).
- [13] T. Matsuoka and K. Shimizu, *Nature (London)* **458**, 186 (2009).
- [14] Q.-J. Hong and A. van de Walle, *Phys. Rev. B* **100**, 140102(R) (2019).
- [15] M. Marqués, M. I. McMahon, E. Gregoryanz, M. Hanfland, C. L. Guillaume, C. J. Pickard, G. J. Ackland, and R. J. Nelmes, *Phys. Rev. Lett.* **106**, 095502 (2011).
- [16] C. J. Pickard and R. Needs, *Nature Mater.* **9**, 624 (2010).
- [17] M.-S. Miao and R. Hoffmann, *Acc. Chem. Res.* **47**, 1311 (2014).
- [18] J. Neaton and N. Ashcroft, *Nature (London)* **400**, 141 (1999).
- [19] K. Takemura and K. Syassen, *Phys. Rev. B* **28**, 1193 (1983).
- [20] D. MacDonald, W. Pearson, and L. T. Towle, *Can. J. Phys.* **34**, 389 (1956).
- [21] V. Subbotin, M. Arnol'Dov, F. Kozlov, and A. Shimkevich, *At. Energ.* **92**, 29 (2002).
- [22] D. R. Burfield, K.-H. Lee, and R. H. Smithers, *J. Org. Chem.* **42**, 3060 (1977).
- [23] T. M. Hunt, T. Hunt, N. Vaughan, and N. Vaughan, *The hydraulic handbook* (Elsevier, Amsterdam, 1996).
- [24] F. Laves and H. Wallbaum, *Z. Anorg. Allg. Chem.* **250**, 110 (1942).
- [25] A. Simon and G. Ebbinghaus, *Z. Naturforsch., B* **29**, 616 (1974).
- [26] S. Desgreniers, S. T. John, T. Matsuoka, Y. Ohishi, and J. T. Justin, *Sci. Adv.* **1**, e1500669 (2015).
- [27] D. R. Anderson, J. B. Ott, J. R. Goates, and H. T. Hall Jr, *J. Chem. Phys.* **54**, 234 (1971).
- [28] L. Yang, X. Qu, X. Zhong, D. Wang, Y. Chen, J. Yang, J. Lv, and H. Liu, *J. Phys. Chem. Lett.* **10**, 3006 (2019).
- [29] A. Dewaele, P. Loubeyre, and M. Mezouar, *Phys. Rev. B* **70**, 094112 (2004).
- [30] C. Prescher and V. B. Prakapenka, *High Press. Res.* **35**, 223 (2015).
- [31] V. Petříček, M. Dušek, and L. Palatinus, *Z. Kristallogr. - Cryst. Mater.* **229**, 345 (2014).
- [32] K. Momma and F. Izumi, *J. Appl. Crystallogr.* **44**, 1272 (2011).
- [33] J. P. Perdew, K. Burke, and M. Ernzerhof, *Phys. Rev. Lett.* **77**, 3865 (1996).
- [34] G. Kresse and J. Hafner, *Phys. Rev. B* **47**, 558 (1993).
- [35] G. Kresse and J. Furthmüller, *Comput. Mater. Sci.* **6**, 15 (1996).
- [36] G. Kresse and J. Furthmüller, *Phys. Rev. B* **54**, 11169 (1996).
- [37] G. Kresse and D. Joubert, *Phys. Rev. B* **59**, 1758 (1999).
- [38] H. J. Monkhorst and J. D. Pack, *Phys. Rev. B* **13**, 5188 (1976).
- [39] A. Togo and I. Tanaka, *Scr. Mater.* **108**, 1 (2015).
- [40] A. D. Becke and K. E. Edgecombe, *J. Chem. Phys.* **92**, 5397 (1990).
- [41] P. W. Stephens, *J. Appl. Crystallogr.* **32**, 281 (1999).
- [42] See Supplemental Material at <http://link.aps.org/supplemental/10.1103/PhysRevB.101.224108> for additional diffraction data.
- [43] M. Winzenick, V. Vijayakumar, and W. B. Holzapfel, *Phys. Rev. B* **50**, 12381 (1994).
- [44] M. Hanfland, I. Loa, and K. Syassen, *Phys. Rev. B* **65**, 184109 (2002).
- [45] W. Holzapfel, *Europhys. Lett.* **16**, 67 (1991).
- [46] N. E. Christensen, *Phys. Rev. B* **32**, 207 (1985).
- [47] L. F. Lundegaard, G. W. Stinton, M. Zelazny, C. L. Guillaume, J. E. Proctor, I. Loa, E. Gregoryanz, R. J. Nelmes, and M. I. McMahon, *Phys. Rev. B* **88**, 054106 (2013).
- [48] B. Böhm and W. Klemm, *Z. Anorg. Allg. Chem.* **243**, 69 (1939).
- [49] M. Frost, A. L. Levitan, P. Sun, and S. Glenzer, *J. Appl. Phys.* **123**, 065901 (2018).
- [50] B. Rousseau and N. W. Ashcroft, *Phys. Rev. Lett.* **101**, 046407 (2008).